Novelties of solid–liquid phase transfer catalyzed synthesis of o-nitrodiphenyl ether

Ganapati D. Yadav*, S. Subramanian

Department of Chemical Engineering, University Institute of Chemical Technology, University of Mumbai, Matunga, Mumbai 400019, India

Abstract

o-Nitrodiphenyl ether is an important intermediate in the fine chemical industry and used in a number of drugs. This ether is typically prepared from o-chloronitrobenzene (OCNB) by condensing with alkali metal phenoxides in toluene or xylene in presence of copper or cuprous chloride and the process requires a high temperature to initiate the formation of cuprous salt of phenol. Once initiated the reaction is exothermic and can sometimes become uncontrolled leading to the formation of tarry masses. In the current work synthesis of o-nitrodiphenyl ether was accomplished by reacting o-chloronitrobenzene with solid potassium phenoxide using tetra-n-butylphosphonium bromide as a catalyst under solid–liquid phase transfer catalysis (S–L PTC). The advantages of S–L PTC are that the reaction is conducted at controllable temperatures, the rates of reaction are increased by orders of magnitude and the reaction is 100% selective, in comparison with the liquid–liquid (L–L) PTC which is very slow and produces by-products. The mechanism based on homogeneous solubilization of solid resulting in the formation of an active ion-pair with the nucleophile was found to prevail in the system. A complete theoretical analysis is done to determine both the rate constant and equilibrium constant from the same set of data. The reaction is intrinsically kinetically controlled.
© 2003 Elsevier B.V. All rights reserved.

1. Introduction

Phase transfer catalysis (PTC) has been applied to over 600 industrial processes in a variety of industries such intermediates, dyestuffs, agrochemicals, perfumes, flavours, pharmaceuticals and polymers [1–3]. A large number of PTC processes use the liquid–liquid (L–L) mode of operation. PTC has been quite successful for C, N, O and S alkylations involving SN_2 type reactions in fine chemical industries, apart from dehydrohalogenations. A few important pharmaceutical applications of PTC are: synthesis of chloramphenicol involving aldol condensation [4], alkylation of phenyl acetonitrile, a precursor for dicyclomine, phenopyridine, oxaldine, etc. [5], N-alkylation of phenothiazine and iminodibenzyl useful for making chlorpromazine and imipramine [6], and O-acylation of estradiol with N,N-bis(2-chloroethyl)carbamoyl chloride [7]. The agrochemical processes using PTC, for instance,

are the synthesis of 3,5-dichloro-α-methyl styrene (dehydrobromination of α-bromo-3,5-dichlorocumene) [8] and in the preparation of fenvalerate, an insecticide (condensation of 4-chloro propylated phenyl acetyl chloride with m-phenoxybenzaldehyde cyanohydrin) [9,10].

o-Nitrodiphenyl ether is a commercially important intermediate which is synthesized by a cumbersome, expensive and polluting method. We would like to report a 100% selective and cheaper process to synthesize o-nitrodiphenyl ether using a solid–liquid (S–L) PTC.

o-Nitrodiphenyl ether is traditionally prepared by reacting aqueous sodium phenoxide with o-chloronitrobenzene in toluene or xylene in the presence of cuprous chloride. Reaction of cuprous salt of phenol (prepared by reacting sodium phenoxide and cuprous chloride), and iodobenzene gives diphenyl ether [11]. Another paper reports the reaction of potassium phenoxide with p-chloro nitrobenzene in refluxing chlorobenzene with copper powder as catalyst. This process is highly exothermic and the reaction sometimes gets out of control [12].

When the halogen exchange of alkoxides is conducted in L–L PTC, there is always a formation of alcohols due to hydrolysis. One of the ways to suppress by—product

* Corresponding author. Tel.: +91-22-2410-2121;
fax: +91-22-2414-5614.
E-mail addresses: gdyadav@yahoo.com, gdyadav@hotmail.com
(G.D. Yadav).

formation and also intensify the rates of reactions of L–L PTC is through the use of solid–liquid PTC. The aqueous phase promoted reactions can thus be totally suppressed and better selectivities obtained. While liquid–liquid PTC involves heterogeneous reaction between two reagents located in an aqueous, and an organic phase, solid–liquid PTC involves reaction of an anionic reagent in a solid phase (usually a salt) with a reactant located in a continuous organic phase. Yadav and Sharma [13] proposed the first mechanistic and kinetic model of solid–liquid PTC for the reaction of benzyl chloride with solid sodium acetate and benzoate, to produce the commercially important benzyl esters, which has been commercialised in India. Apart from our fundamental work on S–L PTC, it has been modelled by Naik and Doraiswamy [14]. The role of small amounts of water, the so-called omega phase, in S–L PTC was analysed in our earlier work [13] including others [1–3] and a rigorous model of S–L PTC with omega phase has been advanced recently [15].

The current work deals with the novelties of 100% selective synthesis of *o*-nitrodiphenyl ether including the kinetic modelling relevant for scale up and reactor design.

2. Experimental

2.1. Chemicals and catalysts

o-Nitrochlorobenzene (ONCB), benzyl triethyl ammonium chloride (BTEAC) and tetrabutyl phosphonium bromide (TBPB) were obtained from Fluka Chemika, CH-9470, Buch, Switzerland. Phenol was procured from Ms. E. Merck India Ltd., Mumbai. India, chlorobenzene from Ms. Thomas Baker (Chemicals) Ltd., Mumbai. Potassium hydroxide AR grade was purchased from S. D. Fine Chemicals, Mumbai. Tetra-*n*-butyl ammonium hydrogen sulphate (TBAHS) and tetra-*n*-butyl ammonium bromide (TBAB) used were obtained from Loba Chemie and also donated by Dishman Chemicals and Pharmaceuticals Ahmedabad, India.

2.2. Experimental procedure

The reaction was studied in a 5 cm. i.d. fully baffled mechanically agitated glass reactor of 150 cm^3 total capacity which was equipped with a six blade-pitched turbine impeller (2 cm diameter) and a reflux condenser. The impeller was located at a distance of 2 cm from the bottom. This arrangement ensured excellent solid–liquid mixing for high mass transfer rates. The assembly was kept in an isothermal bath at the desired temperature and mechanically stirred at a known speed with an electrical motor. Predetermined quantities of reactants and solvent were added to the reactor and the temperature raised to the desired value. The catalyst was added when the temperature reached the set value.

Typically the reaction was carried out as follows. Initially, a suspension of 0.025 mol potassium phenoxide was prepared in situ from 0.025 mol phenol and 0.025 mol potassium hydroxide by heating in chlorobenzene at 110 °C for 1 h. The reaction was very facile. Water was removed by azeotropic distillation and a completely dry suspension of potassium phenoxide was formed in situ. Potassium phenoxide was generated in situ as fine particles in the range of 50–100 μm. The reaction was carried out at the set temperature after the addition of 0.02 mol of OCNB and 3.0 mol% of catalyst on the basis of OCNB. The total volume was made to 45 ml by adding chlorobenzene. A zero time sample was collected and sampling was done periodically to get concentration–time profiles of reactants and products.

The reaction scheme is as given below.
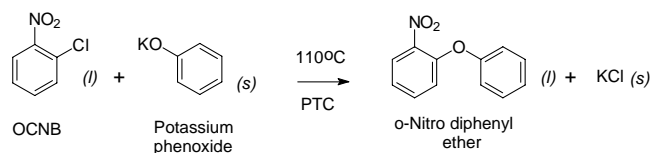
The same reaction under liquid–liquid PTC conditions did not proceed and a very small quantity of *o*-nitro-phenol was formed as the only byproduct.

2.3. Analysis

Analysis was performed on GC (Chemito Gas Chromatograph, model 8510) by using a 2 m × 3.8 mm stainless steel column packed with 10% OV-17 on Chromosorb WHP, coupled with a flame ionisation detector. Synthetic mixtures of the reactant and internal standard were used to calibrate the chromatograms and quantify the data. Upon completion of reaction, the reaction mixture was washed with water to remove unreacted potassium phenoxide and then distilled under reduced pressure to separate the product, which was characterized by GC-MS. Both analyses showed that only *o*-nitrodiphenyl ether was the sole product. A mass balance was also carried out.

3. Results and discussions

Preliminary experiments established that the reaction was facile at 110 °C. To understand the enhanced rates of reaction under these conditions, it was thought worthwhile to study the mechanism and kinetics of this reaction. The reaction under L–L PTC under otherwise similar conditions under reflux conditions is slower by orders of magnitude and leads to the formation of by-products due to hydrolysis of halogen in the benzene ring and also formation of the corresponding ether. These reactions are avoided under anhydrous conditions. Besides, the interfacial area of a liquid–liquid agitated mixture is much lower than the surface area created by fine particles, thereby leading to very high mass transfer rates. Since a typical experiment produced 92% conversion of ONCB, with 100% selectivity to the ether, a further

insight was obtained by studying the effect of various parameters on the rates of reaction.

3.1. Mechanism and kinetic model

The first step in the reaction involves the transport of a reactant anion (substrate, Y^-) from the solid phase to the organic phase by a phase transfer cation (Q^+). This is an organophilic quaternary cation which exchanges the anion (X^-) with the nucleophile phenoxide to form the $[Q^+Y^-] = [Q^+OPh^-]$, which is organophilic and is freely transported to the bulk organic phase. There could be a resistance associated with the transfer of this ion-pair across the liquid film next to solid–liquid interface. The second step involves the reaction of the $[Q^+Y^-]$ with the reactant (RX) located in the organic phase. There are several possibilities by which this reaction can occur. Finally the third step involves the transport of the co-product anion $[X^-]$, the leaving group, by the phase transfer cation to the solid and the transport of another nucleophile $[Y^-]$ into the organic phase. In the

current case, the S–L PTC mechanistic description is the implication that the reaction takes place in anhydrous condition, since both solid and liquid phases were dry. So the formation of the omega phase was discounted.

There are two types of mechanisms for S–L PTC, the homogeneous solubilization mechanism of Yadav and Sharma [13] and heterogeneous solubilization of Naik and Doraiswamy [14] (Fig. 1). In the heterogeneous solubilization, the particles are totally insoluble and the catalyst get adsorbed on to the solid whereas in the case of homogeneous solubilization model, the particles are sparingly soluble in the organic phase and the particle solubility is augmented by the phase transfer agent (Q^+X^-) as shown in Fig. 2. There is an instantaneous exchange of anions and formation of an ion-pair (Q^+Y^-) with the quaternary cation Q^+ with the nucleophile Y^- which diffuses from the solid–liquid interface to the organic phase through the organic film. The particle size goes on decreasing with time due to the reaction in the organic phase. Depending on the relative rate of transfer of Q^+Y^- in the organic film next to the solid and the reaction
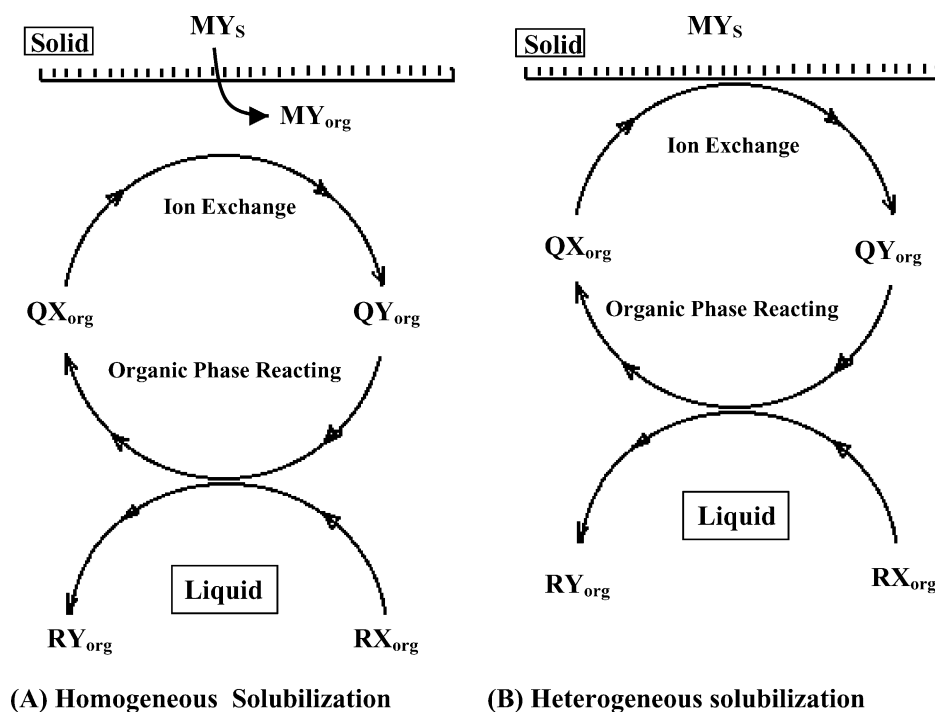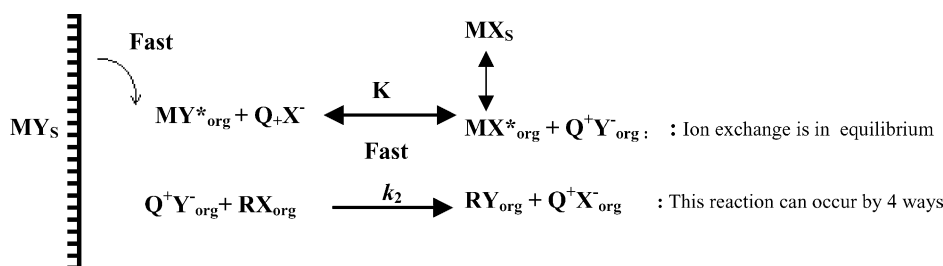

Fig. 1. Mechanism of S–L PTC reaction.

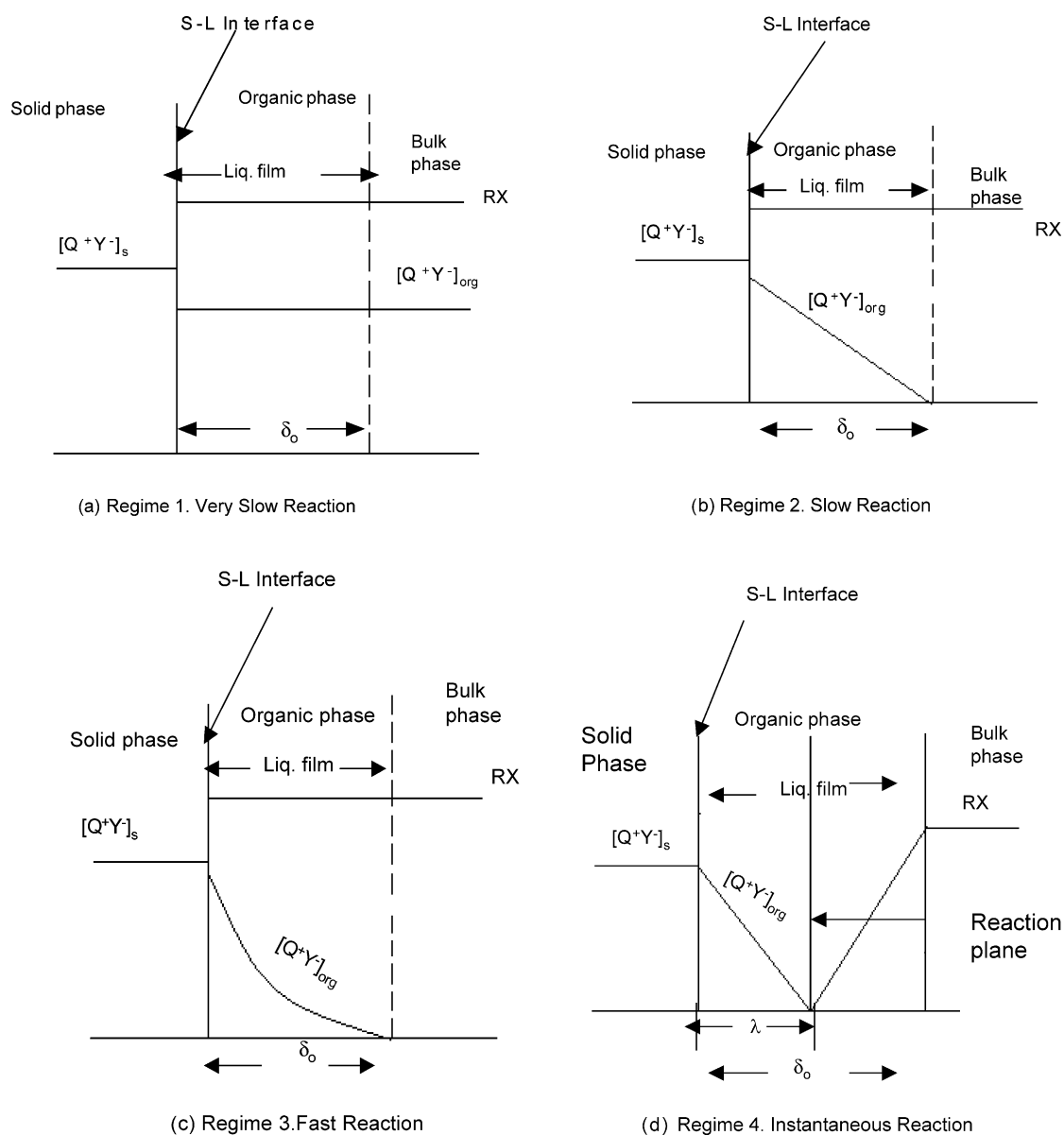Fig. 2. Homogeneous solubilization PTC.

Fig. 3. Typical S–L PTC under homogeneous solubilization: (a) regime 1: very slow reaction. The reaction occurs in the bulk organic phase as a homogeneous reaction. Mass transfer effects are unimportant. (b) Regime 2: slow reaction. The reaction occurs in the bulk organic phase. No free concentration of ion pairs exists in the bulk organic phase. (c) Regime 3: fast reaction. Diffusion of $[Q^+Y^-]_{(org)}$ and its reaction with RX are steps in parallel, and the reaction occurs in the organic liquid film next to the S–L interface. (d) Regime 4: instantaneous reaction. The reaction between $[Q^+Y^-]_{(org)}$ and RX is so fast that they cannot coexist in the organic phase. $[Q^+Y^-]_{(org)}$ diffuses from the L–L interface, and RX diffuses from the bulk organic phase into the organic liquid film and react at a plane Ï from the interface. No free $[Q^+Y^-]_{(org)}$ exists beyond distance λ and no free RX exists beyond distance $(\delta_0-\lambda)$ toward the interface. Note that for simplicity other ion pairs are not shown.

of the species, four different regimes can be identified just like the L–L PTC [16,17]. These are shown in Fig. 3 and the importance of various steps is delineated in the captions.
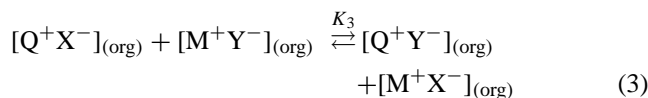
Preliminary experiments suggested that the homogeneous solubilization model (regime 1) illustrated by the SN$_2$ type of reaction of the substrate RX with the nucleophile Y of the solid reactant MY. M$^+$ is the inorganic metallic counter-ion of the nucleophile Y$^-$ was applicable to the current work. The calculations are shown later in Section 3.3. The overall reaction is:

$$RX_{(org)} + MY_{(s)} + [Q^+X^-]_{(org)} \xrightarrow{k_{obs}} RY_{(org)} + MX_{(s)}$$
$$+ [Q^+X^-]_{(org)} \qquad (1)$$
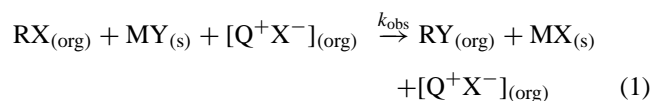
where Q^+ is the quaternary cation of the catalyst. Q^+X^- is a loosely bound ion pair shown in brackets. The solid reactant is in equilibrium with its solution in the organic phase.

$$MY_{(s)} \overset{K_2}{\rightleftharpoons} [M^+Y^-]_{(org)} \qquad (2)$$

The quaternary salt (Q^+X^-) reacts with the dissolved part of the solid reactant in the organic phase.

$$[Q^+X^-]_{(org)} + [M^+Y^-]_{(org)} \overset{K_3}{\rightleftarrows} [Q^+Y^-]_{(org)}$$
$$+ [M^+X^-]_{(org)} \quad (3)$$

$$[M^+X^-]_{(org)} \overset{1/K_4}{\rightleftarrows} M^+X^-_{(s)} \quad (4)$$

The substrate RX reacts with $[Q^+Y^-]$ according to

$$RX_{(org)} + [Q^+Y^-]_{(org)} \overset{k_r}{\rightarrow} RY_{(org)} + [Q^+X^-]_{(org)} \quad (5)$$

The quaternary salt is thus generated repeatedly to catalyze the reaction. However, there is no transfer of the catalyst across the interface as is normally observed in the case of liquid–liquid phase transfer process.

The equilibrium constant K_e which is a sort of a solubility parameter is defined by combining steps (3) and (4) as follows:

$$K_e = \frac{[Q^+Y^-]_{(org)}[M^+X^-]_s}{[Q^+X^-]_{(org)}[M^+Y^-]_s} = \frac{K_2 K_3}{K_4} \quad (6)$$

The rate of reaction for Eq. (5) is given by

$$-\frac{d[RX]_{(org)}}{dt} = k_r[RX]_{(org)}[Q^+Y^-]_{(org)} \quad (7)$$

Therefore,

$$-\frac{d[RX]_{(org)}}{dt} = k_r K_e \frac{[M^+Y^-]_s}{[M^+X^-]_s}[RX]_{(org)}[Q^+X^-]_{(org)} \quad (8)$$

But

$$Q_0 = [Q^+Y^-]_{org} + [Q^+X^-]_{org}$$
$$= \text{total concentration of catalyst in organic phase} \quad (9)$$

Let fractional conversion of RX at time t,

$$X_A = \frac{N_{RX_0} - N_{RX}}{N_{RX_0}} \quad (10)$$

where N_{RX_0} are the initial moles of RX at time $t = 0$

Let

$$M = \frac{N_{MY_0}}{N_{RX_0}} = \text{initial mole ratio of nucleophile to substrate,}$$

From the stoichiometry of the reaction, all terms in Eq. (8) can be written in terms of X_A and Q_0. Separation of variables and integration leads to the following:

$$\int_0^{X_A} \left[\frac{X_A + K_e M - K_e X_A}{K_e(M - X_A)(1 - X_A)} \right] dX_A = k_r Q_0 t \quad (11)$$

This integral is solved by the method of partial fractions to get the following:

$$\left(\frac{M}{M-1} \right) \ln \left(\frac{M - X_A}{M} \right) - \left(\frac{1 - K_e + K_e M}{M - 1} \right) \ln(1 - X_A)$$
$$= k_r Q_0 t \quad \text{for } M \neq 1 \quad (12)$$

Eq. (12) can be further manipulated to the following to extract both K_e and k_r:

$$\left[\frac{\ln\{(M - X_A)/M\}}{\ln(1 - X_A)} \right] - \left[\frac{1 - K_e + K_e M}{M} \right]$$
$$= \left[\frac{(M-1)k_r Q_0}{M} \right] \frac{t}{\ln(1 - X_A)} \quad (13)$$

A plot of $\left[\dfrac{\ln\{(M-X_A)/M\}}{\ln(1-X_A)} \right]$ versus $\dfrac{t}{\ln(1-X_A)}$ should give

$$\text{slope} = \left[\frac{(M-1)k_r Q_0}{M} \right] \text{ and intercept}$$
$$= -\left[\frac{1 - K_e + K_e M}{M} \right] \quad (14)$$

Thus, both K_e and k_r can be obtained from the slope, intercept and from the knowledge of M and Q_0. Further for equimolar quantities of substrate and nucleophile, the following form of the integrated equation results.

$$\left(\frac{X_A}{1 - X_A} \right) + (1 - K_e)\ln(1 - X_A) = k_r Q_0 t$$
$$\text{for } M = 1 \quad (15)$$

Eq. (15) is also manipulated to the following.

$$\left[\frac{X_A/(1 - X_A)}{\ln(1 - X_A)} \right] + (1 - K_e) = k_r Q_0 \frac{t}{\ln(1 - X_A)} \quad (16)$$

A plot of $[(X_A/1 - X_A)/\ln(1 - X_A)]$ versus $t/\ln(1 - X_A)$ will give a straight line with slope equal to $k_r Q_0$ and intercept equal to $(1 - K_e)$.

The validation of the above model was verified by conducting several experiments.

3.2. Effect of various catalysts

Four different catalysts, benzyltriethylammonium chloride (BTEAC), tetra-*n*-butylphosphoniumbromide (TBPB), tetra-*n*-butylammonium hydrogensulfate (TBAHS) and tetra-*n*-butyl ammonium bromide (TBAB) were selected for the reaction under otherwise similar concentrations of catalysts at 110 °C and 1000 rpm (Fig. 4). Out of these, TBPB gave the maximum rates of reaction and conversion. The reasons for better activity of TBPB is that majority of it exits in the active form $[Q^+OPh^-]_{(org)}$. Quaternary phosphonium salts are more stable than the quaternary ammonium salts thereby maintaining higher concentration of $[Q^+Y^-]$ in the organic phase. Thus, further experiments were conducted with this catalyst. The selectivity to the ether was 100%.

3.3. Effect of speed of agitation

The reaction was carried out at four different speeds of agitation with TBPB as catalyst. There was a significant increase in the conversion from 500 to 1000 rpm but it
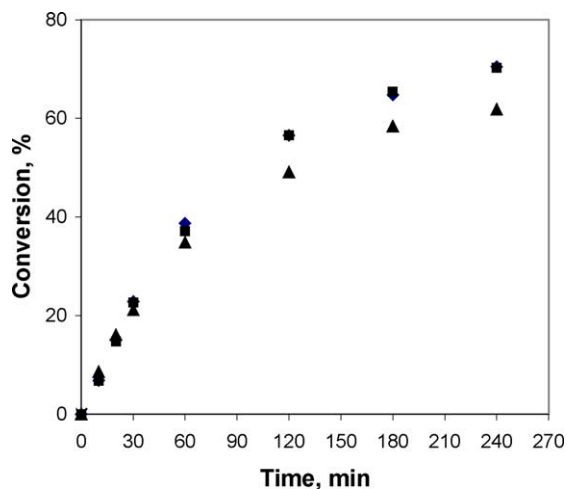
Fig. 4. Effect of catalyst type, OCNB: 0.02 mol; potassium phenoxide: 0.025 mol; catalyst loading: 3.0 mol% of OCNB; chlorobenzene: to make total volume 45 ml; temperature: 110 °C. (◆) TBEAC, (■) TBAB, (▲) TBAHS and (×) TBPB.

was almost constant at 1000 rpm and 1200 rpm. This indicated the absence of external mass transfer resistance beyond 1000 rpm. All subsequent reactions were carried out with 1000 rpm while assessing the effect of other variables on the rate of reaction. A calculation was done to find out if the theory of mass transfer with reaction could be invoked to find the locale of reaction in the absence of mass transfer resistance and to which regime the system belonged (see Fig. 3).

The observed initial rate of reaction, for a typical experiment was equal to $1.06 \times 10^{-7} \, \mathrm{mol \, cm^{-3} \, s^{-1}}$ whereas the rate of mass transfer was estimated from the knowledge of

solid–liquid mass transfer coefficient (k_{SL-A}), particle surface area ($a_p = 600 \, \mathrm{cm^{-1}}$) and the solubility of potassium phenoxide in chlorobenzene ($3.78 \times 10^{-5} \, \mathrm{mol/cm^3}$). The solid–liquid mass transfer coefficient (k_{SL-A}) was found from the Sherwood number ($k_{SL-A} d_p / D_A = 2$). A limiting value of Sherwood was taken as 2 since the particles were very fine. The Wilke–Chang equation was used to calculate the bulk diffusivity. The mass transfer rate was equal to $7.95 \times 10^{-5} \, \mathrm{mol \, cm^{-3} \, s^{-1}}$, which is 750 times greater than the rate of reaction. Thus, the observed reaction rate was slower than the mass transfer rate, and the organic phase was always saturated with the ion-pair [Q^+OPh^-], thereby making it as a pseudo-first-order reaction belonging to regime 1 and is given by Eq. (5). That is, the reaction occurred in the bulk liquid phase and not in the film surrounding the solid particle.

3.4. Effect of catalyst loading

The concentration of the catalyst was varied from 4.44×10^{-6} to $3.5 \times 10^{-5} \, \mathrm{mol/cm^3}$org. It was observed that as the concentration was increased, the conversion increased, but above a concentration of $2.22 \times 10^{-5} \, \mathrm{mol/cm^3}$, there was no further increase in the conversion. This suggested that the reaction rate was fast and thus mass transfer of [Q^+OPh^-] from the liquid film to the bulk liquid was controlling beyond $2.22 \times 10^{-5} \, \mathrm{mol/cm^3}$. Here, the rate of mass transfer was less than the rate of reaction (so-called regime 2). The validity of Eq. (13) was tested. Appropriate plots were made for $M = 1.25$ as shown in Fig. 5. There is an excellent fit for different values of catalyst concentration. The average values of k_r and K_e were obtained as $430 \, \mathrm{cm^3 \, mol^{-1} \, min^{-1}}$ and 14.28, respectively.
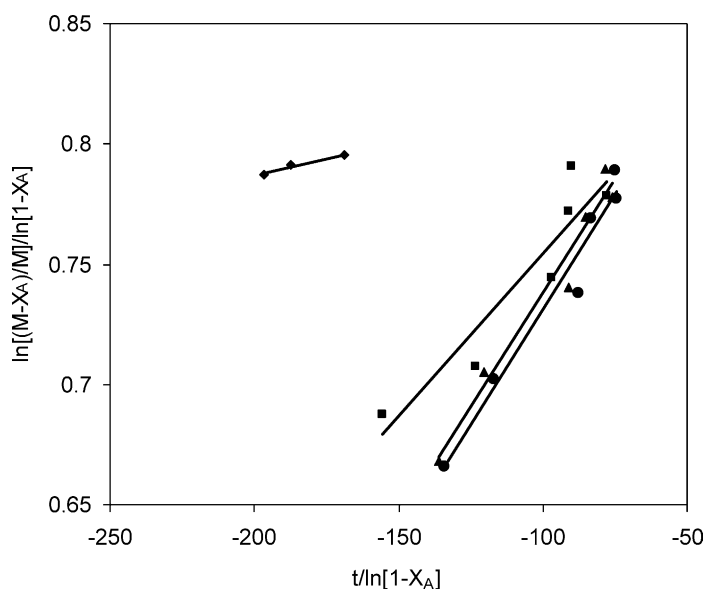

Fig. 5. Effect of catalyst concentration, OCNB: 0.02 mol; potassium phenoxide: 0.025 mol; chlorobenzene: to make total volume 45 ml; speed of agitation: 1000 rpm; temperature: 110 °C. Average $k_r = 430 \, \mathrm{cm^3 \, mol^{-1} \, min^{-1}}$, $K_e = 14.28$, (◆) $4.44 \times 10^{-6} \, \mathrm{mol/cm^3}$, (■) $1.33 \times 10^{-5} \, \mathrm{mol/cm^3}$, (▲) $2.22 \times 10^{-5} \, \mathrm{mol/cm^3}$ and (●) $3.5 \times 10^{-5} \, \mathrm{mol/cm^3}$.
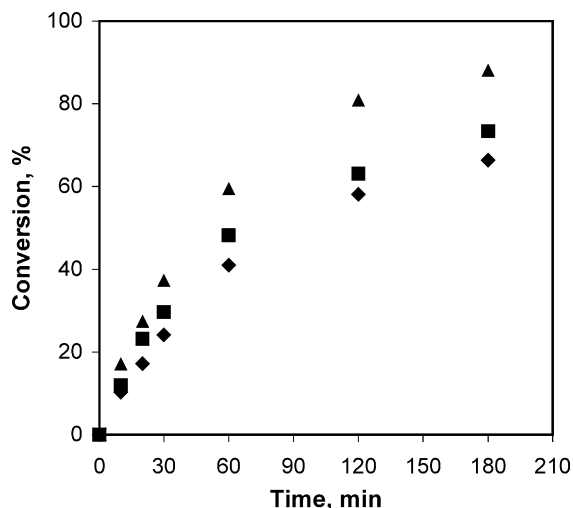
Fig. 6. Effect of various mole ratios of OCNB to potassium phenoxide, OCNB: 0.02 mol (fixed); chlorobenzene: to make total volume 45 ml; speed of agitation: 1000 rpm; TBPB: 5.0 mol%; temperature: 110 °C. (◆) 1:1, (■) 1:1.25, (▲) 1:2 and (×) 1:2.5.

3.5. Effect of mole ratio

The effect mole ratio of OCNB to potassium phenoxide was studied from 1:1 to 1:2.5, keeping the total volume of the reaction mass constant at 45 ml with chlorobenzene by keeping the quantity of OCNB constant at 0.02 mol. The catalyst loading was kept at 2.22×10^{-5} mol/cm^3. The conversion was found to increase marginally and remained the same at the mol ratios of OCNB to potassium phenoxide of 1:2 and 1:2.5 and the conversion was 92% with 100% selectivity to the ether (Fig. 6). This is obvious from the fact that
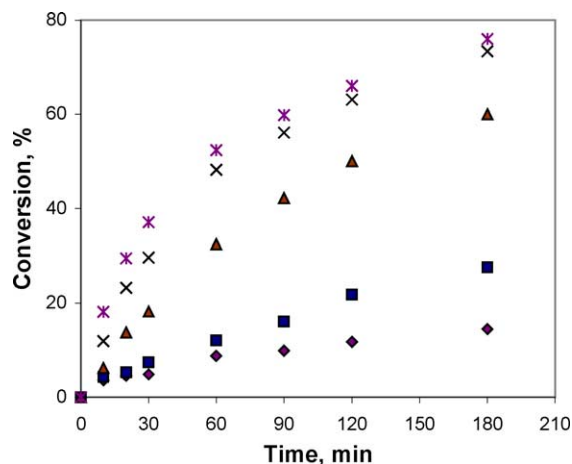

Fig. 8. Effect of temperature, OCNB: 0.02 mol; potassium phenoxide: 0.025 mol; chlorobenzene to make total volume 45 ml; speed of agitation: 1000 rpm; TBPB: 5.0 mol%. (◆) 90 °C, (■) 100 °C, (▲) 105 °C, (×) 110 °C and (✶) 120 °C.

the concentration of the ion-pair $[Q^+OPh^-]$ in the organic phase remains constant as is evident from Eqs. (2) and (3). So further addition of potassium phenoxide does not help in enhancement of the rate of reaction. Eqs. (13) and (16) were used for $M = 1$ and $M \neq 1$ to make the plots to validate the theory as shown in Fig. 7. This also demonstrates that there is a very good fit.

3.6. Effect of temperature

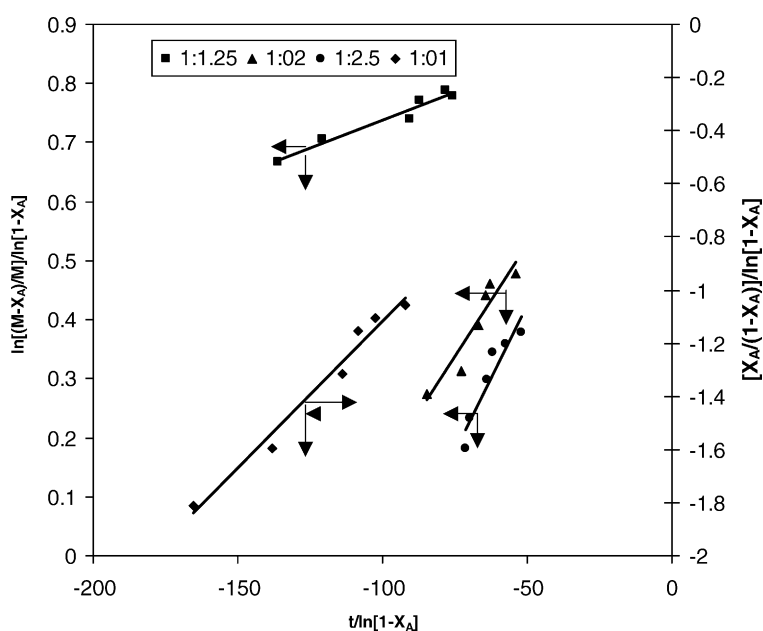The effect of temperature was studied under otherwise similar reaction conditions from 90–120 °C (Fig. 8). It was

Fig. 7. Determination of k_r and K_e for various mole ratios of OCNB to potassium phenoxide, OCNB: 0.02 mol (fixed); chlorobenzene: to make total volume 45 ml; speed of agitation: 1000 rpm; TBPB: 5.0 mol% of OCNB; temperature: 110 °C.
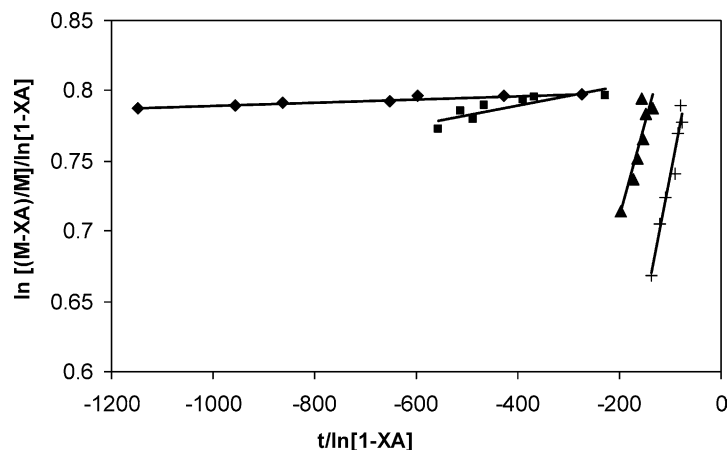
Fig. 9. Validation of model at different temperatures, OCNB: 0.02 mol; potassium phenoxide: 0.025 mol; chlorobenzene: to total volume 45 ml; speed of agitation: 1000 rpm; TBPB: 5.0 mol%. (◆) 90 °C, (■) 100 °C, (▲) 105 °C and (×) 110 °C.

found that the conversion increased substantially with increase in temperature. However, there was marginal increase in conversion at 120 °C over than at 110 °C, bringing into play the mass transfer effects. The same theory was again validated at all temperatures up to 110 °C (Fig. 9). Thus, Arrhenius plot was made and the activation energy calculated as 10.05 kcal/mol, which suggested that the reaction was kinetically controlled.

4. Conclusions

o-Nitrodiphenyl ether is an important intermediate in the fine chemical industry and it is industrially prepared from o-chloronitrobenzene (OCNB) by condensing with alkali metal phenoxides in toluene or xylene in presence of copper or cuprous chloride and the process requires a high temperature to initiate the formation of cuprous salt of phenol. Once initiated the reaction is exothermic and can sometimes become uncontrolled leading to the formation of tarry masses. A process was developed to prepare o-nitrodphenyl ether from OCNB and solid potassium phenoxide with 100% selectivity by using solid–liquid phase transfer catalysis. The S–L PTC process is more intensified and far better than the L–L PTC. Effects of various parameters were studied on the rate of reaction. Tetra-n-butylphosphonium bromide was found to be the best catalyst. A complete theoretical analysis of the process was carried out to explain the observed rate data. Both equilibrium constant and rate constant could be calculated from the same set of data. The apparent activation energy is 10.05 kcal/mol.

Acknowledgements

References

[1] C.M. Starks, C. Liotta, M. Halpern, Phase Transfer Catalysis: Fundamentals, Applications, and Perspectives, Chapman and Hall, New York, 1994.
[2] Y. Sasson, R. Neumann (Eds.), Handbook of Phase Transfer Catalysis, Blackie Academic and Professional, London, 1997.
[3] E.V. Dehmlow, S.S. Dehmlow, Phase Transfer Catalysis, third ed., VCH, New York, 1993.
[4] M. Koch, A. Magni, US Patent 4,501,919 (1985);
    M. Koch, A. Magni, Chem. Abstr. 102 (1985) 204296.
[5] L. Lindblom, M. Elander, Pharmaceut. Tech. 4 (1980) 59.
[6] S.J. Schmolka, H. Zimmer, Synthesis (1984) 29.
[7] H.J. Fex, S.K. Kristensson, A.R. Slamvik, Ger. Offen. 629 (2) (1978) 657.
[8] K. Henneke, H. Diehn, K. Wedemeyer, US Patent 4,594,467 (1986).
[9] R.A. Sheldon, P. Been, D.A. Wood, R.F. Mason, Ger. Offen. 708 (2) (1977) 590.
[10] S. Subramanian, New Insight Into Catalytic Application for Pharmaceutical Syntheses, Ph.D. (Tech.) Thesis, University of Mumbai, Mumbai, India, June 2002.
[11] I. Iwamoto, et al., Chem. Express. 8 (1) (1993) 57–60.
[12] R.Q. Brewster, T. Groening, Org. Syn. Coll. 2 (1943) 445.
[13] G.D. Yadav, M.M. Sharma, Ind. Eng. Chem. Process Res. Dev. 20 (1981) 385–390.
[14] S.D. Naik, L.K. Doraiswamy, Chem. Eng. Sci. 52 (1997) 4533.
[15] G.D. Yadav, Y.B. Jadhav, Langmuir 18 (2002) 5995–6002.
[16] G.D. Yadav, B.V. Haldavanekar, J. Phys. Chem. A. 101 (1997) 36–48.